INJURY THRESHOLD FOR SAGITTAL PLANE ROTATIONAL INDUCED DIFFUSE AXONAL INJURIES

J. Davidsson[1], M. Angeria[2] and M. G. Risling[2]

[1] Division of Vehicle Safety, Applied Mechanics, Chalmers University of Technology, Göteborg
[2] Experimental Traumatology, Department of Neuroscience, Karolinska Institute, Stockholm

ABSTRACT

Sagittal plane rotational acceleration induced diffuse axonal injury threshold was investigated using an animal model in which the heads of the rats were exposed to selected rotation accelerations. Post-trauma survival times ranged from 3 to 120 h. Numerous S100 serum concentrations, brain tissue stained for β-Amyloid Precursor Protein (β-APP), and probes for Cyclooxygenase 2 (COX2) mRNA were used to detect affected nerve cells, decaying axons, and cytoskeletal changes, respectively. Scaling laws were applied to estimate injury thresholds for the human brain.

Confocal imaging revealed bands of β-APP-positive axons in the corpus callosum and its edges in animals exposed to rotational accelerations >1.1 Mrad/s2. Similarly, for COX2 presence and S100 concentrations at >0.9 Mrad/s2, the numbers of stained cells in the cortex and hippocampus and the concentrations increased. The data clearly indicate that the rat brain is injured at a specific rotational acceleration. Scaled to that of humans this would be 10 krad/s2 with a duration of 4 ms.

Key words: Brain, Animal model, Diffuse Axonal Injury

TRAUMATIC BRAIN INJURIES (TBI), which are a major public health problem, represent approximately 60% of all deaths in hospitals among children and young adults in the western world (Melvin et al., 1993). Among survivors these injuries are often irreversible, causing long term pain and disability. Although TBI can be associated with skull fractures, it commonly occurs without fractures (Gennarelli and Thibault 1982). About 40% of the TBI patients admitted to hospitals are non-focal injuries (Wismans et al., 2000), usually referred to as distributed brain injuries (DBI); the primary cause of these injuries is head rotation (Holbourne, 1943) which often occurs in traffic related and military assault accidents.

A large number of studies have hypothesized that the resulting strains in the brain tissue are the primary cause of neurological deficiencies following DBI (Adams et al. 1989; Margulies and Thibault 1992; Margulies et al. 1990; Povlishock 1992; Strich 1961; Zhang et al. 2004). It has been suggested that the severity of the injury correlates with the amplitude of the angular acceleration (Abel et al. 1978; Margulies and Thibault 1992; Ono et al. 1980), or with the resulting angular velocity (Kleiven et al 2007). Duration of the impact has been reported to affect the injury type; short duration results in focal injury, while long duration impacts result in DBI (Margulies and Thibault 1992; Ono et al. 1980).

There are at least four categories of DBI: diffuse axonal injury (DAI); diffuse hypoxic, anoxic or ischemic injury; diffuse swelling; and diffuse vascular injury. The DAI, which is form of distributed axonal injury (AI) is the most common type of DBI; it commonly results in unconsciousness or death (Gennarelli et al. 1982, Melvin et al., 1993). The DAI pathology, which is characterized by perturbations to the axoplasmic transport along the length of axons (Povlishock and Jenkins, 1995), is likely to cause axonal swelling or degeneration which can reduce the functionality or disconnect the axons from their existing networks (Povlishock, 1992). It has been reported that DAI are localized in the subcortical white matter, grey-white matter interface and corpus callosum (Smith and Meaney, 2000, Ommaya 1984 and Gennarelli et al., 1982) and at points of attachment, such as blood vessels and cranial nerves (Viano 1997).

Diffuse axonal injury is commonly a result of inertial induced loads; intracranial motions arise when the skull is accelerated and the brain mass, due to its inertia, lags behind or continues its motion relative the skull. Hence, the risk of DAI is highly dependent on brain mass (Margulies and Thibault

1992). It has also been shown, in experiments with monkeys, that the incidence and degree of diffuse axonal injury correlated, although indirectly, with the direction of the head acceleration: coronal plane angular acceleration was the direction that caused the longest lasting coma, while sagittal plane angular accelerations and oblique accelerations produced coma for a shorter period (Gennarelli et al., 1982).

The Head Injury Criterion (HIC) is the primary measure of head and brain injury risk used today. It has been heavily criticized mainly because it only takes linear acceleration into account (Newman et al., 1980, Ono et al., 1980, Gennarelli et al., 1982). To provide an improved injury criterion that also predicts the risk of DAI, a correlation between global head rotational acceleration and injury outcome should be established. For the head rotation in the horizontal plane, extensive work has been carried out; Margulies and Thibault (1992) suggested limits which were a combination of rotational acceleration and resulting head rotational velocity. For head rotations in the coronal plane, Xiao-Sheng et al. (2000) exposed rats to 2 ms long rotational accelerations, after which they observed axonal swelling and bulblike protrusions on the axons in the medulla oblongata, midbrain and corpus callosum. In two other studies by Ellingson et al. (2005) and by Fijalkowski et al. (2007), rats were exposed to higher rotational accelerations (368 krad/s²) in the coronal plane than in the study by Xiao-Sheng and colleagues. Despite the higher accelerations, the rats suffered from classical concussion injuries with minimal histological abnormalities. Finally, for head rotation in the sagittal plane that causes DAI, only limited data is available; for concussion injuries, Ommaya et al. (1967) scaled and combined data from experiments on some animal species and proposed a sagittal plane angular acceleration threshold of 1.8 krad/s^2. For gliding contusions, Löwenheim (1975) suggested that the tolerance value in the sagittal plane should be 4.5 krad/s^2. Ewing et al. (1975) used volunteers to show that no adverse effects were observed in instrumented volunteers exposed to head accelerations of 2.7 krad/s^2 in the sagittal plane. In other studies, real life accidents were used to shed some light on global head rotational acceleration limits. In most of these studies the heads were exposed to a combination of oblique linear and multi axis rotational accelerations.

To conclude, data suggesting DAI thresholds for sagittal plane rotation is limited, hence the main purpose of this study is to estimate, by using an animal brain trauma model that produces graded injury, the global head rotational acceleration in the sagittal plane, which causes diffuse axonal injury.

MATERIALS AND METHODS

The materials and methods used in this study are briefly presented below. A thorough presentation is available in Davidsson et al. (2009).

ANIMALS: Sixty-two male Sprague-Dawley rats weighing 0.415 kg in average, between 0.352 kg and 0.518 kg, were deeply anaesthetized by a 2.4 ml/kg intra-abdominal injections of a mixture of 1ml Dormicum® (5 mg/ml Midazolan, Roche), 1 ml Hypnorm® (Janssen) and 2 ml of distilled water. Thereafter the subjects were given 0.2 ml/kg intra-muscular injections every 0.5 h until the trauma and following surgery was carried out. The work was performed in accordance with the Swedish National Guidelines for Animal Experiments, which was approved by the Animal Care and Use Ethics Committee in Umeå.

In all animals, a midline incision was made through the skin and periosteum on the skull vault, and parts of the frontal, nose and parietal bones were freed from adherent tissue. The exposed bone was treated with 15% phosphate acid for 3 minutes, thoroughly rinsed with tempered distilled water, and dried for 3 minutes with an air drier providing air at 37°C. The exposed bone was then gently sanded prior to glueing (Super-Bond C & B; Sun Medical Co., Shiga, Japan) of a curved aluminium plate, denominated the *skull cap,* and shaped to match the contour of the exposed skull (35 mm long and 2-9 mm wide). The dental glue was allowed to cure for min 15 minutes at 37° C.

EXPERIMENTAL SETUP: Prior to experiments, an *attachment plate* was fastened by means of two screws to the *skull cap* previously glued to the rat skull bone (Fig. 1). Then the *attachment plate* was inserted and secured to a *rotating bar* that can rotate freely around a horizontal axis. The resulting pre-trauma position of the head was slightly flexed and the brain centre of gravity located about 6.5

mm above the centre of rotation. This is equivalent to a centre of rotation located 1 mm below the head base and 5 mm forward of the front of the foramina magnum.

Forty-seven of the animals were traumatized: during trauma a solid brass weight, denominated the *striker (weight 0.040 kg),* hit the polyurethane bumper on the striker target (aluminium plate 6 mm thick and 15 mm wide) and the impulse produced subjected the animal heads to a short sagittal plane rearward rotational acceleration for about 0.4 ms. This was followed by a rearward rotation at near constant velocity and, finally, the heads came to a stop by a deceleration of about 25% of the initial acceleration (Fig. 2). The entire trauma, which caused the head and neck to extend 25°, represents a forehead impact to the steering wheel in a frontal car collision or to the ground in a fall accident. Fifteen animals served as sham exposed controls. The rotational acceleration magnitude was selected by modifying the *striker* speed which was varied by means of modifying the air pressure in a specially designed air driven *accelerator* (CNC-Process AB, Hova, SWEDEN).

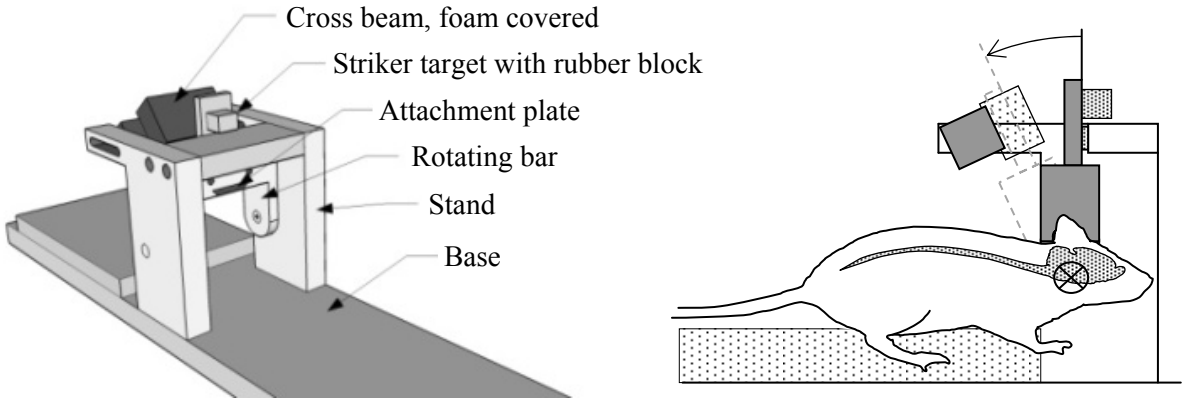

Fig. 1 - Diagram of the test device used to accelerate the head of the rat rearward in the sagittal plane; oblique frontal view and side view of the head.

INSTRUMENTATION, DATA ACQUISITION AND ANALYSIS: An Endeveco Isotron 2255B-01 piezoelectric accelerometer, with integrated electronics and resonance frequency above 300 kHz, was mounted on the *rotating bar* at a radius of 36.5 mm from the centre of rotation and connected to a Endeveco 4416B signal conditioner. The analogue signal was digitized and captured by means of a National Instrument DAQ Card 6062 at 200 kHz. The rotational acceleration data was filtered using SAE J211 CFC3000 (5000 Hz). In a few of the tests, the accelerometer signal was also captured by means of an oscilloscope at 5 MHz; no apparent difference between DAQ card data and oscilloscope data was observed.

A chronograph (SKAN PRO1 Series 3) was used to capture the velocity of the striker.

In some experiments, side views of the head trauma were recorded by a Redlake video at 20 000 f/s with a resolution of 120×68 pixels. Before the experiments, film targets and a grid (spacing 5×5 mm) were fitted to both the stand and rotating bar. Oblique frontal views of the trauma were also recorded to monitor the rigidity of the head-to-test rig attachment.

Angular velocity and displacement were numerically integrated from the unfiltered acceleration data and compared with the high speed data for accuracy.

SCALING ROTATIONAL ACCELERATION, VELOCITY AND DURATION: The injury thresholds obtained in the experiments with rats in this study were scaled to those of humans using equations initially suggested by Holbourn (1943), Ommaya et al. (1967) and Margulies et al. (1985), later modified by Gutierrez et al. (2001). Their work provides a relationship between rotational acceleration (α) and the mass (m):

$$\alpha_H = \alpha_R \left(\frac{m_R}{m_H} \right)^{2/3}$$

where *H* represents human and *R* represents rat. Provided human and rat brains have the similar properties, the mass in the equation can be replaced by the cube of the ratio of humans to rat length. The relation between rotational acceleration (α), duration (t) and resulting velocity (v) can then be estimated by:

$$\alpha_H = \alpha_R \left(\frac{L_R}{L_H} \right)^2 \qquad t_H = t_R \left(\frac{L_H}{L_R} \right) \qquad v_H = v_R \left(\frac{L_R}{L_H} \right)$$

DISSECTION, IMUNOHISTOLOGY, IN-SITU HYBRIDIZATION, AND SERUM ANALYSIS: Post-trauma survival times were varied from 2 h to 5 days (Table 2) for two reasons; first, the initial ethical approval only permitted short survival times; second, the authors preferred to assess the effect on the brain tissue as soon after the trauma as possible to avoid other secondary effects associated with the trauma or preparation of the animal prior to trauma. The reason for increasing the survival time, among others, was to evaluate whether β-APP reactivity was a function of survival time.

During the sacrifice of the animals, venous blood was collected from the right ventricle of the heart with a Safety-Lock needle and SST II blood collection system containers (BD Vacutainer®) which include a clot activator and gel for serum separation. For most subjects two 3.5 ml containers were filled and treated according to the instructions provided with the system. Serum was frozen immediately after centrifugation and stored at -20° deg until the analysis.

The brains were then dissected and placed in a brain blocker and split into a frontal, middle and occipital units which were fresh frozen on dry ice. Coronal 14 μm cryostat sections from these regions were cut and incubated to study the accumulation of beta-amyloid precursor protein (β-APP). The tissue was also incubated with Neurofilaments (NF), which is a major element of the cytoskeleton supporting the axon cytoplasm. In situ hybridization was conducted to asses the presence of Cyclooxygenase 2 (COX2) which is an enzyme responsible for formation of important biological mediators; prostanoids. Normally COX2 is undetectable, but it is known to be abundant in cells at sites of inflammation and has been suggested to correlate with cell death.

In the analysis, two brain sections from each of the three regions in the brain, frontal, middle and occipital, were chosen arbitrarily, and NF, β-APP and COX-2 reactivity was assessed with either a confocal microscope or traditional white light microscope. For β-APP and COX-2, the analysis also included scoring according to a grading schema (Table 1).

Table 1. Grading of β-APP and COX-2.

Grade	*Number of β-APP-positive axons per section*	*Shape and dimension of β-APP-positive axons*	*Intensity of COX-2 silver staining per section*	*Localization of the COX-2 positive cells*
0	Only slight β-APP stains in cell body	–	Sometimes visible	Distributed regardless of tissue type
1	50 - 100	Small but asymmetric	Visible in 10 x microscope	Localized to cell bodies
2	100 - 200	Large and asymmetric	Visible in 1x microscope, bright contrast underlying tissue	Localized to cell bodies
3	>200	Large and some extended along the axon	Visible macroscopically and overshadowing tissue behind	Localized to cell bodies

Two of the S100 proteins, S100A1B and S100BB, found in the central nervous system glial cells, are known to be released into body fluids following trauma (Ingebrigtsen et al. 2000). In the current study, serum S100BB levels and the total S100B (S100A1B and S100B) levels were assessed with two immunoassays (S100 EIA and S100B EIA, Can Ag Diagnostics AB, Gothenburg, Sweden). Only serum samples that exhibited minimal hemolysis and from animals that were anesthetized for 2.5 h prior to sampling were included in the study.

RESULTS

TEST PROTOCOL: The magnitude of the rotational acceleration used for the first experiments in this study was based on a suggested injury threshold for humans. Traditional scaling laws and geometrical properties of the human (Gutierrez et al. 2001) and rat brain were used to estimate the loading in the first few experiments (Table 2). In some of the first tests, the *skull cap* came loose during trauma or the skull bone fractured during the trauma. After a few tests the load magnitude was reduced; macroscopic injuries decreased and nearly all *skull caps* remained firmly fixed to the skull bone during the trauma. In the first few experiments the skull cap was larger than in the following experiments; the location of the first skull cap relative to the head depended on whether the nasal shape and whether the bone could fully be denuded. Hence, the centre of rotation varied more in the first few experiments than in the rest of the series. Not all animals were used for serum and histological tissue analysis. Of those experiments intended to be used in this analysis, seven were excluded because the *skull cap* came loose during trauma. Four animals died during trauma from excessive neck angulations which probably caused fatal brain stem or upper spine injuries (not evident in all animals). Also, three animals were eliminated due to trauma related skull bone fractures. In about eight experiments the animals died before, during or after trauma, possibly as a consequence of the introduction of anaesthetics.

ROTATIONAL ACCELERATION AND VELOCITY CHANGE: The resulting head angular acceleration lasted for about 0.4 ms, and filtered peaks were approximately 0.4 to 2.1 Mrad/s^2 in this study (Fig. 2 and Table 2). After 10 to 15 degrees of head rotation, the striker target made contact with a high density Tempur foam, and the rotating bar and attached head came to halt after a total of about 2 ms at an angle of 20 to 25° deg. There appears to be a linear correlation between resulting angular velocity and peak angular acceleration (R = 0.93, n = 46). Only the striker velocity was varied, which means that the duration of the acceleration remained rather constant while peak rotational acceleration varied (Fig. 2).

In the experiments, the centre of rotation was not perfectly in the brain centre of gravity; hence the brain was exposed to a combination of rotational and linear accelerations. The maximum linear acceleration in the brain centre of gravity ranged from 3600 to 7400 m/s^2 for the three experiments included in Fig. 2.

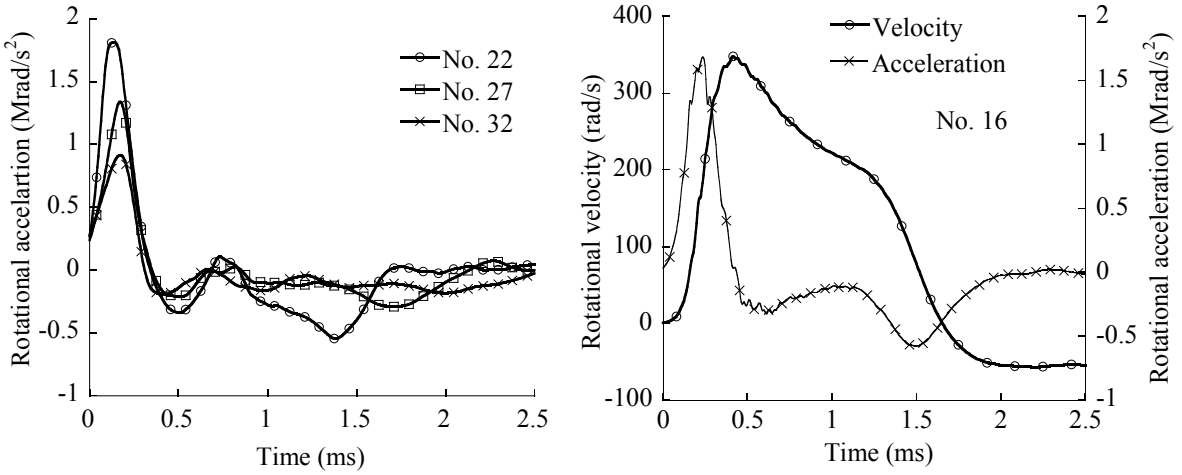

Fig. 2 - Left: Rotating bar accelerations obtained in experiments that exhibited widespread, slight or no β-APP reactivity. Right: Rotational acceleration and integrated rotational acceleration.

For evaluation of the recorded linear acceleration and subsequent calculation of rotational acceleration, images of the rotating bar during trauma were recorded using a high speed video. Time from start to stop of the angulations of the head, obtained from video analysis, matched that of the accelerometer data. Resulting peak angulations of the rotating bar during the trauma, as estimated by

double integration of the rotational acceleration, were also consistently about 20 degrees and matched those of the video data.

Table 2. Test conditions and results (blank: not analysed; (-): not possible to analyse; NR: not recorded).

No.	*Rot. Acc. (Mrad/s²)*	*Rot. Vel. (rad/s)*	*Survival time (h)*					*APP*			*COX2*			*S100B total; batch (ng/L)*		*S100BB; batch (ng/L)*		
			2.0-2.5	*3.3*	*24*	*72*	*120*	*Frontal*	*Middle*	*Occipital*	*Frontal*	*Middle*	*Occipital*	*1*	*2*	*1*	*2*	*3*
11	1.79	369	*					3	1	0	2	3	2	-	-	-	-	-
13	2.09	404	*					3	1	0	2	3	2	-	-	-	-	-
14	0	0	*					0	0	0	0	1	0	-	-	-	-	-
16	1.68	348		*				3	2	1	2	2	2	-	-	-	-	-
19	1.92	359		*				3	2	2	3	2	3	-	-	-	-	-
20	1.73	296		*				3	1	2	3	3	3	-	-	-	-	-
22	1.81	361	*					3	2	2	2	2	3	-	-	-	-	-
23	1.48	273	*					3	1	1	2	2	3	-	-	-	-	-
25	1.46	269	*					1	0	0	2	2	1	2068		973		1092
26	1.44	258	*					2	2	0	2	2	1	-	-	-	-	-
27	1.34	257	*					1	0	0	2	2	2	-	-	-	-	-
28	1.61	278	*					3	1	0	0	1	1	-	-	-	-	-
29	1.54	265	*					3	2	0	1	1	2	681	937	301		249
30	1.13	220	*					1	1	0	0	1	2	-	-	-	-	-
31	0.94	208	*					1	0	0	0	1	0	479	647			210
32	0.92	195	*					2	0	1	0	0	0	284				123
33	1.50	281	*					3	1	3	1	1	1	-	-	-	-	-
34	0.70	-	*					0	0	0	0	0	0				49	73
35	0.51	133	*					0	0	0	0	0	0	150				93
36	2.10	304	*					3	2	1	1	2	2	843				526
38	1.30	-	*					3	2	1	1	2	2	228		127	136	165
39	0.98	188	*					2	0	0	1	1	1	167			90	108
40	1.34	214	*					2	1	2	2	2	2	-	-	-	-	-
41	1.06	197	*					1	0	0	-	-	-	-	-	-	-	-
42	1.15	221	*					0	1	1	1	2	1	192	315			160
43	1.15	177	*					2	2	0	-	-	-	313		156		165
44	0.37	61	*					0	0	0	0	0	0		144		36	71
45	0.63	125	*					0	0	0	0	0	0		243		53	90
46	0.99	198	*					2	0	1	0	0	0	284				129
47	0.91	202	*					0	0	0	1	2	1	-	-	-	-	-
48	0	0	*					0	0	0	0	0	0			100		78
49	0	0	*					0	0	0	0	0	0					58
50	0	0	*					0	0	0	0	0	0				36	54
71	1.04	201			*			2	1	3				229	618			
72	1.43	273			*			3	2	3				153	266			
73	1.41	263			*			3	3	2				179				
75	0	0			*			0	0	0				134	284			
76	0	0			*			0	0	0				176				
85	1.45	-			*			-	-	-	-	-	-		370			
86	1.53	287			*			-	-	-	-	-	-		198			
87	1.64	275			*			-	-	-	-	-	-		198			
88	1.50	286			*			-	-	-	-	-	-		188			
89	0	0			*			-	-	-	-	-	-		306			
90	0	0			*			-	-	-	-	-	-		316			
92	0	0			*			-	-	-	-	-	-		158			
93	0	0					*	0	0	0								
94	1.76	310					*	3	0	0								
97	1.41	276					*	3	1	1								
102	1.36	267					*	3	1	0								
106	0	0					*	0	0	0								
107	1.66	276					*	3	1	0								
108	1.80	264					*	3	0	0								
109	0	0					*	0	0	0								
112	1.11	228			*			3	1	0								
115	1.06	200				*		3	0	1								
116	1.28	278				*		3	0	1								
117	0	0				*		0	0	0								
120	1.53	280			*			3	-	-		-	-					
122	0	0			*			0	-	-		-	-					
123	1.88	294			*			3	-	-		-	-					
124	0	0			*			0	-	-		-	-					
125	1.87	295			*			3	-	-		-	-					

MACROSCOPIC INJURY: During sacrifice, hemorrhages were visual in the foramen magnum region; subdural and subarachnoid hemorrhages were observed on the superior cortex surface in about half of the exposed animals. A few animals suffered from hemorrhages in the vicinity of the olfactory bulb. A few intracranial hemorrhages were noted in the animals that had been subjected to rotational acceleration close to 2 Mrad/s^2.

MICROSCOPIC INJURY: Bands of β-APP-positive axons, i.e. axons with reduced axioplasmic transport, were seen in the border between the cortex and the corpus callosum in nearly all animals exposed to head rotational trauma at 1.1 Mrad/s^2 or higher (Fig. 3, 4 and 6). For many of the exposed animals, β-APP was also found in the thalamus, on the lower edges of the corpus callosum, in the corpus callosum, the caudate putamen, the commisure, and in the hippocampus regions. Most animals exhibited similar numbers of and intensity of β-APP-positive axons on the right and left hemispheres. No obvious difference in the number of β-APP-positive axons could be observed for survival times between 2.5 and 3.3 h. The size and extent of β-APP-positive axons appeared to increase when the survival time was 24 h compared with 3.3 or 2.5 h. No β-APP reactivity was found in the sham exposed animals.

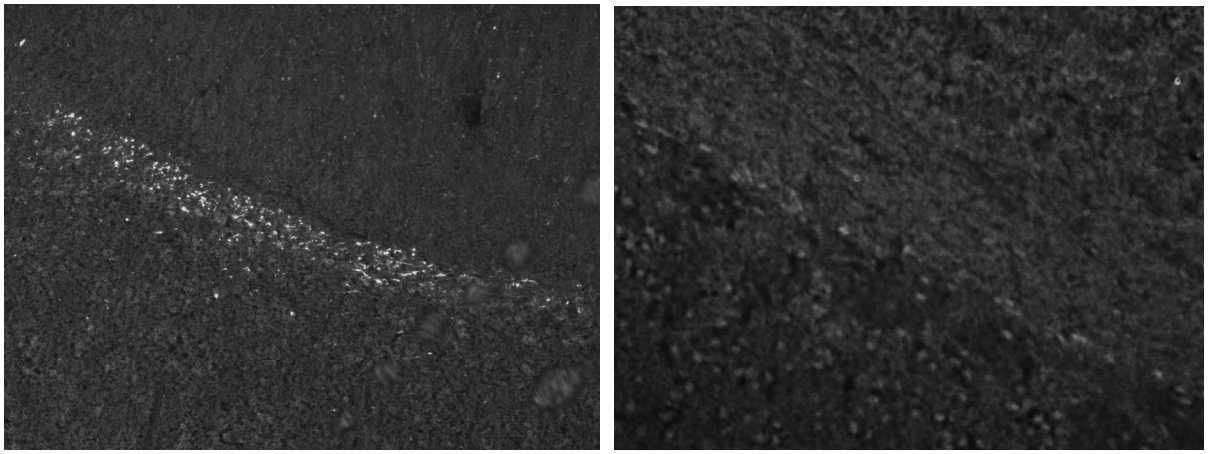

Fig. 3 - Confocal images of coronal plane frontal sections of the corpus callosum (upper part) and subcortical white matter (lower part) incubated with β-APP: exposed (No. 73, resolution 10x) and sham exposed animal (No. 76, resolution 20x) to the left and right, respectively.

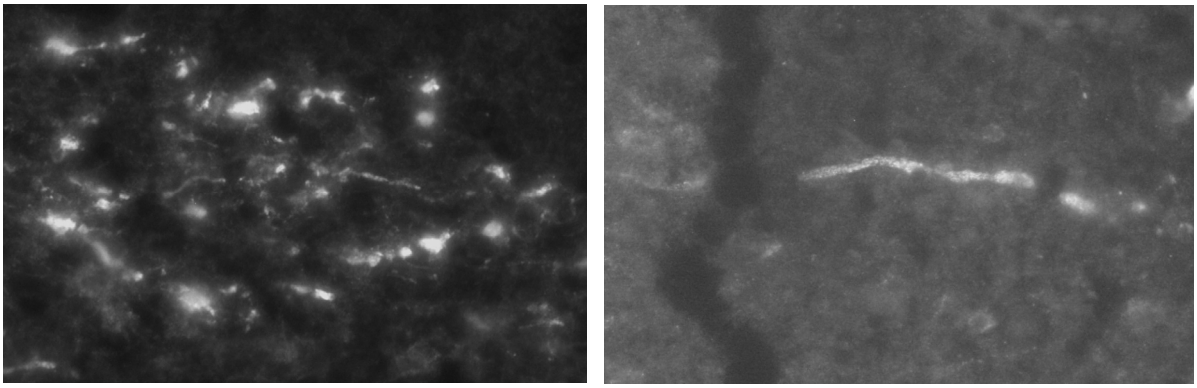

Fig. 4 - High resolution (60x) confocal coronal plane images of β-APP stained tissue, frontal region, illustrating axonal injury (No. 73 and 112).

The highest intensity and density of β-APP-positive axons were found in the frontal sections when compared with middle and occipital sections. For survival times 3.3 h or less the average β-APP score was two and for survival times 24 h or longer the score was three. In contrast, the β-APP scores were below one for both middle and occipital sections regardless of survival time.

In the frontal sections, the β-APP-positive axons were most proliferate on the boundary between the cortex and the corpus callosum (forceps minor); they could also be found in the caudate putamen

and the body of the corpus callosum (forceps minor). The extensions of the β-APP positive axons in the lateral direction varied from one animal to another. In the middle brain sections, small diameter β-APP positive axons were found in some animals in the hippocampus region, in the edge of the corpus callosum and in the vicinity of the lateral ventricle.

For the NF marker, very limited changes were observed and only in the animals that survived 72 h post trauma. Commonly axonal end-bulb formations could be observed but not satisfactorily documented.

For the COX2-probe, few or no cells were labelled in normal or sham operated animals. In animals subjected to trauma a distinct rise of COX2 could be detected at a large number of places in the cortex and hippocampus after rotational acceleration of above 0.9 Mrad/s^2 (Fig. 5 and 6). In the frontal sections, the COX2 was found mainly in the cingulated cortex and in the lateral regions of the cortex. In the middle sections, reactivity was found in the dentate gyrus, putamen/hippocampus region, and lateral regions of the cortex. In the occipital sections mainly the lateral regions of the cortex exhibited COX2 positive cells.

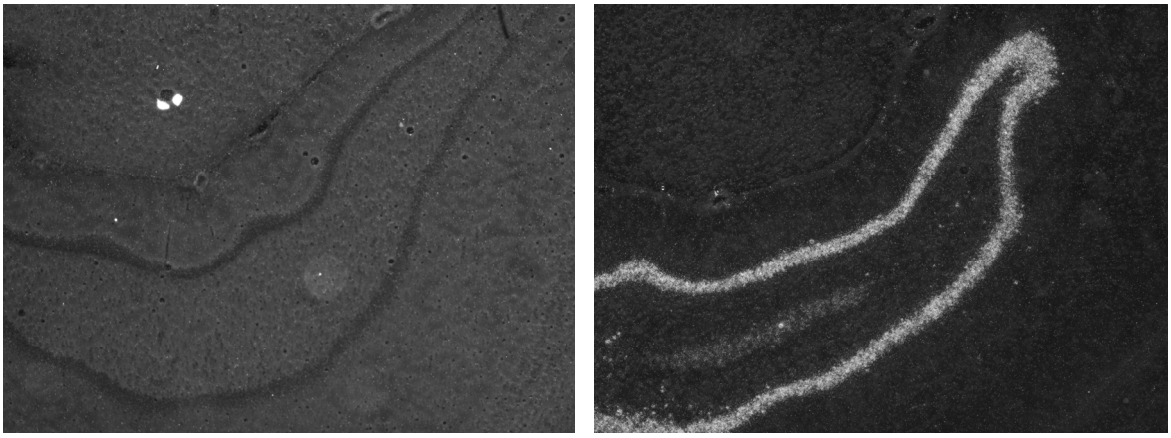

Fig. 5 - Images, captured in optically white light, of coronal plane occipital sections of the Dentate Gyrus stained for Cox2. Left: animal exposed to a 0.7 Mrad/s^2 rotational acceleration (No. 34); Right: animal exposed to a 1.9 Mrad/s^2 rotational acceleration (No. 22), 4x magnification.

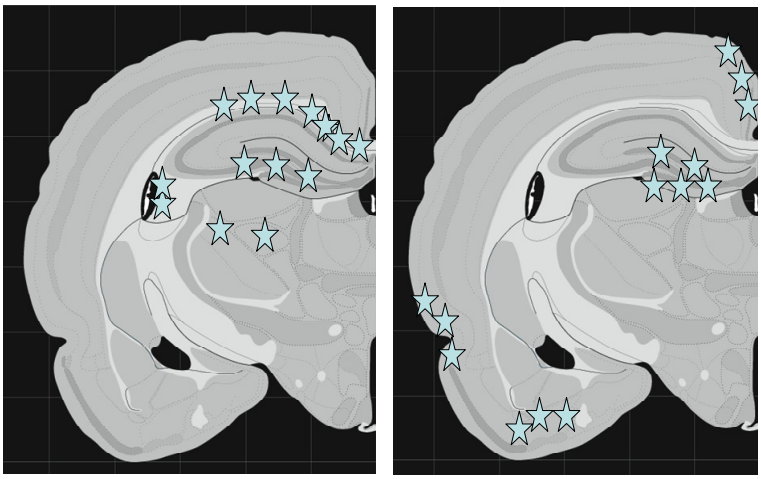

Fig. 6 - Schematics of the middle coronal section of the rat brain. Left: Stars indicating localization of β-APP -positive axons. Right: Stars indicating localization of cells with high intensity of COX2.

The average levels of β-APP-positive axons and COX2 intensity, as subjectively determined according to the grading scheme previously presented (Table 1), increase with rotational acceleration (Fig. 7, Table 2). A clear dose-response pattern can be observed; for β-APP-positive axons the increase starts at 1.1 Mrad/s^2 and for COX2 intensity the increase starts at around 0.9 Mrad/s^2. Moreover, the animals that survived 24 h after trauma exhibited the highest average intensity of β-APP, in comparison with all other survival times, for levels of trauma above 1 Mrad/s^2.

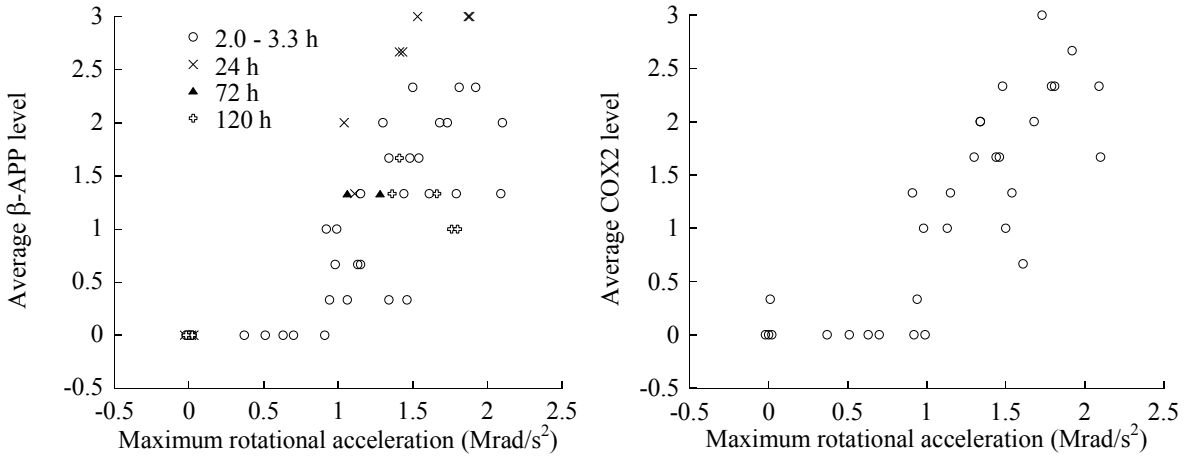

Fig. 7 - β-APP and COX2 levels as a function of maximum rotational acceleration. Note that in the left plot, 12 sham exposed controls are included that all exhibited zero level β-APP. Also, in the right plot three sham exposed controls are included that all exhibited zero level of COX2.

Two repeated analyses of the total S100B level revealed an increase at head acceleration above approximately 0.8 Mrad/s^2 (Fig. 8). Three repeated analyses of S100BB serum levels showed an increase as a function of maximum rotation at about 0.9 Mrad/s^2.

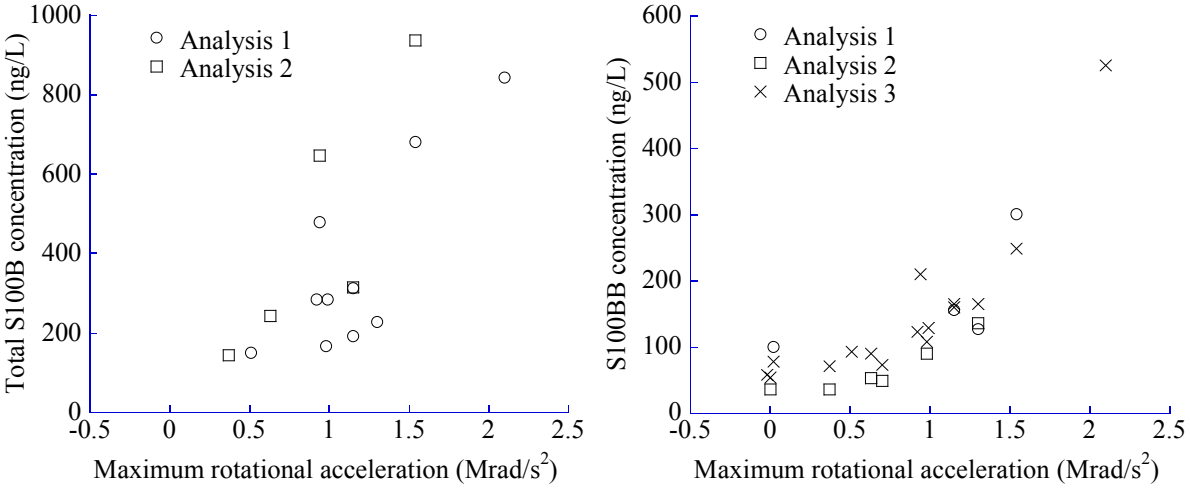

Fig. 8 - Repeated measurements of total S100B and S100BB as a function of maximum acceleration after 2-3.3 h survival time. Extremely high values are not depicted for clarity (No. 25).

RAT AND HUMAN BRAIN DIMENSIONS: In this study the axonal injury threshold, which was obtained in experiments on rats, was scaled to that of humans using scaling laws and brain dimensions measured during the experiments and from the literature (Table 3).

Table 3. Rat and human brain dimensions: rat brain dimension recorded in the current experiments and human brain dimensions obtained from the literature.

Brain dimensions	*Rat (S.D.)*	*Human*
Brain length, including the cerebellum (mm)	22.2 (0.6)	165.0
Brain length, excluding the cerebellum (mm)	15.9 (0.5)	165.0
Height, including the cerebellum (mm)	9.3 (0.5)	140.0
Height, excluding the cerebellum (mm)	9.3 (0.5)	96.0
Characteristic radius, incl. the cerebellum (mm)	7.9	76.3
Characteristic radius, excl. the cerebellum (mm)	6.3	65.3

DISCUSSION

The experimental data reveal that the injury threshold for axonal injury (AI) in the rat brain, due to rearward rotational acceleration, was 1.0 Mrad/s^2 when that pulse duration was 0.4 ms. The scaled representative values for humans were estimated to be 10 krad/s^2 and 4 ms. The scaled rotational velocity change were estimated to be 19 rad/s. These values were estimated using a characteristic radius: (brain length + brain height)/4. The injury threshold range for humans, due to the use of brain lengths and heights with and without the cerebellum, is between 9.3 and 10.7 krad/s^2.

MACROSCOPIC INJURY: In the initial stage of this study, hemorrhages were observed in the foramen magnum region of some of the animals after trauma. To reduce these, to allow reduction effects of excessive hemorrhages, the neck extension was limited to approximately 20 degrees. Also, the mounting position of the skull cap had an effect on these injuries; when the head centre of rotation was shifted forward there were more deaths immediately after trauma or hemorrhages in the brainstem region. No change in the incidence of hemorrhages in the other regions of the brain was observed when the resulting head angle was reduced or centre of rotation shifted rearward. Similarly, only an insignificant correlation between extent of hemorrhages and rotational acceleration was observed: No hemorrhages were found in unexposed control animals, but they were observed in animals exposed to rotational trauma above 0.6 Mrad/s^2.

MICROSCOPIC INJURY: In this study, we have shown that the presence of β-APP positive axons and COX2 stained nerve cells in the brain and the concentration of S100 in serum increased steadily, following a 0.9 - 1.1 Mrad/s^2 sagittal plane rearward rotational acceleration of the rat brain. Since all three markers become apparent and abundant in a rather narrow acceleration interval, it may be suggest that the three markers indicate one single type of brain tissue injury. This injury would most likely be injuries to the axons, but could also be a combination of axonal injuries and contusion injuries to the surface of the brain.

We anticipated more pronounced NF changes, i.e. clear indication and high abundance of reticular bulbs in connection with β-APP-positive axons and contusion injuries near the brain surface were expected. Possibly, reticular bulbs and contusion injuries may be more clearly shown by using other markers or NF for longer survival times.

In this study β-APP was used to assess risk of axonal injury in the brain tissue following rotational trauma and not the traditional staining method which used stains to identifying reticular bulbs. However, numerous studies have shown that β-APP will rather rapidly accumulate after an axon injury at the site of injury; hence it is useful to use β-APP to identify axonal injury shortly after the insult (Gentleman et al., 1993, Blumbergs et al., 1994). Further, Maxwell et al. (1993) suggested that axonal injury is a secondary effect that requires at least 6 h to develop. The authors suggested that an axonal injury takes place due to a chemical cascade which initiates the primary injury to the axolemma. However, the results of the current study suggest that axons are directly affected by the trauma. Here, the intense and early onset of β-APP is most likely a consequence of the insult to the axon itself and not a secondary effect of the insult.

DIFFUSE AXONAL INJURY: In this study the largest number of β-APP-positive axons was found in the edges of and inside the corpus callosum. The localization of the affected axons in this study partly resembles those commonly reported in the literature following DAI Grade I: characterized by microscopical axonal injuries mainly in the corpus callosum and the parasagittal white matter (Adams et al. 1989). The near absence of positive axons in the white matter of the cerebral hemispheres in this study may reflect species differences or does not appear following the type of trauma used here. It has also been reported that DAI is associated with lesions in the brain stem and cerebellum (DAI Grade 3). Here the presence of AI in the brain stem and the cerebellum was not analysed. However, changes to an intermediate filament protein, glial fibrillary acidic protein, were noticed in some of the traumatised animals in the upper brainstem region.

Some studies classify DAI according to the presence of neuropathological changes and the frequency and duration of unconsciousness following trauma (Ono et al. 1980, Gennarelli et al. 1982). In this study the severity of the concussion was not assessed for two reasons: first, the skull cap was

made of aluminium, which would reduced the reliability of result obtained in an EEG study; and second, EEG needles had either to be very tightly secured to the skull bone to withstand the forces during trauma or had to be removed before trauma and reinstalled afterwards. For these reasons, a separate study is to be undertaken in which the EEG measurement procedure is adopted and developed to assess presence and level consciousness following trauma.

Based on the histological findings in this study we are confident that the model used in this study produce DAI since distributed axonal injuries are produced in representative regions of the brain and other injuries are produced in the brainstem. Future studies will further categorize the type of injury produced by the trauma model used in this study.

SCALING INJURY THRESHOLD: The new DAI threshold is only valid for rats and must be scaled prior to use in conjunction with models of the human. The mass of the rat brain is only a fraction of that of humans, which is why the inertia induced strains and stresses are also only a fraction of those in a human brain. These differences were scaled for. Some additional differences between rat brains and human brains, which are likely to affect the relation and, thereby, the scaled injury threshold for humans are listed.

- The proportions of the rat brain are different from those of the human, e.g. the cerebellum is located posterior in the rat, while it is located below in the humans, and the scaled threshold is highly dependent on the measure used (Table 3).
- The surface of the brain of the rat is not folded as in humans. Strain concentrations are probably less common in the rat brain; a consequence of this may be that humans are injured at a lower acceleration threshold than was estimated in this study.
- Localized differences in brain tissue stiffness across the brain will results in stress concentrations. These differences most likely vary between species and may result in differences in injury localization and, thus the effect of the inertia forces.

FUTURE STUDIES: In the near future the following studies are recommended.

- The level of impairment and behavioural changes after trauma should be assessed.
- The risk of DAI as function of peak head rotational acceleration, duration and resulting rotational velocity in the sagittal plane should be determined.
- Peak rotational acceleration values, reported in this study, are dependent on selected filter class and hence the appropriate filter class to be used in studies of rotational acceleration induced brain injuries in the rat needs to be assessed and applied.
- The effect on scaling imposed by differences between the human and the rat using FE-models of the rat and human brain should be introduced.

CONCLUSIONS

We conclude that the data generated in this study reveal that the axonal injury threshold in the rat, due to rearward rotational acceleration, is about 1.0 Mrad/s^2 when the pulse duration is 0.4 ms. We also conclude that the animal model produces axonal injuries mainly in the corpus callosum and on the upper and lower boundaries of the corpus callosum, commonly reported in studies of DAI.

Finally, we suggest that the threshold for DAI for humans exposed to sagittal plane rearward rotation, using traditional scaling laws and typical dimensions of the rat and the human brains, is an acceleration of 10 krad/s^2 when the duration is 4 ms or the angular velocity change is 19 rad/s.

We also acknowledge that traditional scaling laws introduce uncertainty, hence a combination of experimental work and extensive use of detailed FE models of the experiments will produce the most reliable diffuse brain injury threshold for humans.

FORWARD

The study was funded by APROSYS SP 5, the Swedish Armed Forces and Vinnova, Sweden.

REFERENCES

Abel, J., M., Gennarelli, T.A. and Segawa, H. (1978) Incidence and Severity of Cerebral Concussion in the Rhesus Monkey Following Sagittal Plane Angular Acceleration, Proc. of the 22nd Stapp Car Crash Conf.,780886, 35-53.

Adams, J. H., Doyle, D. and Ford, I. (1989) Diffuse axonal injury in head injury: definition, diagnosis and grading. Histopathology, 15, 49–59.

Blumbergs, P. C., Scott, G., Manavis, J., Wainwright, H., Simpson, D. A., and McLean, A. J. (1994) Staining of amyloid precursor protein to study axonal damage in mild head injury. Lancet, 15;344(8929): 1055-6.

Davidsson, J., Angeria, M. and Risling M.G. (2009) A New Device to Produce Sagittal Plane Rotatinal Induced Diffuse Axonal Injuries, In preparation for J. of Trauma.

Ellingson, B. M., Fijalkowski, R. J., Pintar, F. A., Yoganandan, N. And Gennarelli, T. A. (2005) New mechanism for inducing closed head injury in the rat. Biomed. Science Instrumentation, 41:86-91.

Ewing, C. L., Thomas, D. J., Lustick, L., Becker, E. and Williams, G. (1975) The Effect of the Initial Position of the Head and Neck on the Dynamic Response of the Human Head and Neck to -Gx Impact Acceleration, Proc. of the 11th Stapp Car Crash Conf., 751157, 487-512.

Fijalkowski, R. J., Stemper, B. D., Pintar, F. A., Yoganandan, N., Crowe, M. J. and Gennarelli, T. A. (2007) New Rat Model for Diffuse Brain Injury Using Coronal Plane Angular Acceleration, J. of Neurotrauma, 24:1387-1398.

Gennarelli, T. A. and Thibault, L. E. (1982) Biomechanics of subdural Hematoma. J. Trauma, 22, 680-686.

Gennarelli, T.A., Thibault, L.E., Adams, J.H., Graham, D.I., Thompson, C.J. and Marcincin, R.P. (1982) Diffuse axonal injury and traumatic coma in the primate. Annals of Neurology, 12(6), 564-574.

Gentleman, S. M., Nash, M. J., Sweeting, C. J., Graham, D.I. and Roberts, G. W. (1993) Beta-amyloid precursor protein (beta APP) as a marker for axonal injury after head injury. Neurosci Lett. Oct 1;160(2):139-44.

Gutierrez, E., Huang, Y., Haglid, K., Bao, F., Hansson, H.A., Hamberger, A. and Viano, D. (2001) A new model for diffuse brain injury by rotational acceleration. J. Neurotrauma, 18, 247-257.

Holbourn, A. H., (1943) Mechanics of head injuries. Lancet, 2, 438-441.

Ingebrigtsen, T., Romner, B., Marup-Jensen, S., Dons, M., Lundqvist, C., Bellner, J., Alling, C. and Børgesen, S. E. (2000) The clinical value of serum S-100 protein measurements in minor head injury: a Scandinavian multicentre study. Brain Inj., 14:1047-1055.

Kleiven, S. (2007) Predictors for Traumatic Brain Injuries Evaluated through Accident Reconstructions. Proc, of the 51st Stapp Car Crash Conf., Vol. 51, 07S-27.

Löwenhielm, P. (1975) Mathematical simulation of gliding contusions. J. Biomech., 8(6):351-6.

Margulies, S. S., Thibault, L. E. and Gennarelli, T. A. (1985) A Study of Scaling and Head Injury Criteria using Physical Models Experiments. IRCOBI, 13-15.

Margulies, S. S., Thibault, L. E. and Gennarelli, T. A. (1990) Physical model simulations of brain injury in the primate. J. of Biomechanics, 23(8), 823-836.

Margulies, S. S. and Thibault, L. E. (1992) A proposed tolerance criterion for diffuse axonal injury in man. J. of Biomechanics, 25 (8), 917-923.

Maxwell, W.L., Watt, C., Graham, D.I. and Gennarelli, T.A. (1993) Ultrastructural evidence of axonal shearing as a result of lateral acceleration of the head in non-human primates, Acta Neuropathology, 86(2), 136-144.

Meaney, D. F., Smith, D. H. and Shreiber, D. I. (1995) Biomechanical analysis of experimental diffuse axonal injury. J. Neurotrauma , 12, 689-694.

Melvin, J., Lighthall, W.J. and Ueno, K. (1993).Accidental Injury, Biomechanics and Prevention. Springer-Verlag New York. ISBN: 0-387-97881-X.

Newman, J. A. (1980) Head injury criteria in automotive crash testing, Proc. of the 24th Stapp Car Crash Conf., 801317, 703-747.

Ommaya, A. K., Yarnell, P., Hirsch, A. E. and Harris, E. H. (1967) Scaling of Experimental Data on Cerebral Concussion in Sub-Human Primates to Concussion Threshold for Man. Proc. of the 11st Stapp Car Crash Conf., 670906, 73-80.

Ommaya, A. K. (1984) The Head: Kinematics and Brain Injury Mechanisms. In: B. Aldman and A. Chapon, The Biomechanics and Impact Trauma, Amsterdam, Elsevier. 117-125

Ono, K., Kikuchi, A., Nakamura, M., Kobayashi, H. and Nakamura, N. (1980) Human head tolerance to sagittal impact reliable estimation deduced from experimental head injury using subhuman primates and human cadaver skulls. Proc. of the 24th STAPP Car Crash Conf., 801303, 101-160.

Povlishock, J. T. (1992) Traumatically induced axonal injury: pathogenesis and pathobiological implications. Brain Pathol. Jan;2(1):1-12.

Povlishock, J. T. and Jenkins, L. W. (1995) Are the pathobiological changes evoked by traumatic brain injury immediate and irreversible? Brain Pathol., Oct;5(4):415-26.

Smith, D. H. and Meaney, D. F. (2000) Axonal Damage in Traumatic Brain Injury, The Neuroscientist, 6 (6), 483-495.

Strich, S. J. (1961) Shearing of Nerve Fibres as a Cause of Brain Damage due to Head Injury. Lancet, 2, 443.

Viano, D. C. (1997) Brain Injury Biomechanics in Closed-Head Impact. Karolinska Institute, Solna.

Wismans, J., Janssen, E., Beusenberg, M. and Bovendeerd, P. (2000). Injury bio-mechanics. Course book w5-pp3-4.3, Eindhoven Technical University.

Xiao-Sheng, H., Sheng-Yu, Y., Xiang, Z., Zhou, F. and Jian-ning, Z. (2000) Diffuse axonal injury due to lateral head rotation in a rat model. J. Neurosurg, Oct;93(4): 626-633.

Zhang, L., Yang, K.H. and King, A.I. (2004) A Proposed New Injury Tolerance for Mild Traumatic Brain Injury. J. of Biomechanical Engineering 126:226-236.